PHILOSOPHICAL TRANSACTIONS B

royalsocietypublishing.org/journal/rstb

Review

Cite this article: Howarth C, Mishra A, Hall CN. 2021 More than just summed neuronal activity: how multiple cell types shape the BOLD response. *Phil. Trans. R. Soc. B* **376**: 20190630.
http://dx.doi.org/10.1098/rstb.2019.0630

Accepted: 22 September 2020

One contribution of 10 to a theme issue 'Key relationships between non-invasive functional neuroimaging and the underlying neuronal activity'.

Subject Areas:
neuroscience, cognition

Keywords:
BOLD fMRI, neurovascular coupling, neurometabolic coupling, astrocyte, interneuron, endothelial propagation

Authors for correspondence:
Clare Howarth
e-mail: c.howarth@sheffield.ac.uk
Anusha Mishra
e-mail: mishraa@ohsu.edu
Catherine N. Hall
e-mail: catherine.hall@sussex.ac.uk

†These authors contributed equally to this work.

THE ROYAL SOCIETY PUBLISHING

More than just summed neuronal activity: how multiple cell types shape the BOLD response

Clare Howarth[1,†], Anusha Mishra[2,†] and Catherine N. Hall[3,†]

[1]Department of Psychology, University of Sheffield, Sheffield S1 2LT, UK
[2]Department of Neurology, Jungers Center for Neurosciences Research, and Knight Cardiovascular Institute, Oregon Health and Science University, Portland, OR 97239, USA
[3]School of Psychology, University of Sussex, Brighton BN1 9RH, UK

CH, 0000-0002-6660-9770; AM, 0000-0002-3642-5049; CNH, 0000-0002-2316-7714

Functional neuroimaging techniques are widely applied to investigations of human cognition and disease. The most commonly used among these is blood oxygen level-dependent (BOLD) functional magnetic resonance imaging. The BOLD signal occurs because neural activity induces an increase in local blood supply to support the increased metabolism that occurs during activity. This supply usually outmatches demand, resulting in an increase in oxygenated blood in an active brain region, and a corresponding decrease in deoxygenated blood, which generates the BOLD signal. Hence, the BOLD response is shaped by an integration of local oxygen use, through metabolism, and supply, in the blood. To understand what information is carried in BOLD signals, we must understand how several cell types in the brain—local excitatory neurons, inhibitory neurons, astrocytes and vascular cells (pericytes, vascular smooth muscle and endothelial cells), and their modulation by ascending projection neurons—contribute to both metabolism and haemodynamic changes. Here, we review the contributions of each cell type to the regulation of cerebral blood flow and metabolism, and discuss situations where a simplified interpretation of the BOLD response as reporting local excitatory activity may misrepresent important biological phenomena, for example with regards to arousal states, ageing and neurological disease.

This article is part of the theme issue 'Key relationships between non-invasive functional neuroimaging and the underlying neuronal activity'.

1. Introduction

The blood oxygen level-dependent (BOLD) signal in functional magnetic resonance imaging (fMRI) is used as a surrogate measure of neuronal activity. However, because it is not caused directly by neuronal activity but by the disruption of the magnetic field by deoxyhaemoglobin in the blood, the BOLD signal is influenced by several factors beyond neuronal activity. These factors include the geometry of the vascular bed with respect to the magnetic field [1], the concentration of haemoglobin in the blood, blood volume and the oxygenation state of the blood. While the oxygenation state of the blood can be altered by systemic factors such as cardiac rhythm and breathing [2], oxygenation state within the brain is set by the balance between the extraction of oxygen from the blood to fuel increased metabolism (neurometabolic coupling), and the supply of freshly oxygenated blood to an active brain region owing to the dilation of local blood vessels (neurovascular coupling, producing functional hyperaemia). In this review, we examine the contribution of different cell types to these two processes and, therefore, to the BOLD signal to better understand what a regional change in BOLD reveals about the underlying neuronal activity.

2. Neurovascular coupling

(a) Why does neurovascular coupling exist?

The brain is energetically expensive, accounting for 20% of the body's resting energy consumption [3]. In the cerebral cortex, the largest component of this energy is used to fuel the sodium–potassium ATPase, which reverses passive ion fluxes during the action and synaptic potentials to maintain ionic electrochemical gradients [4,5]. Despite this high demand, the brain stores very low levels of energy substrates required for ATP production, largely in the form of glycogen. Compared with other organs, the brain's glycogen storage capacity is small, being approximately one-tenth of that of skeletal muscle and one-thirtieth that of the liver (from values reported in [6–10]). Therefore, the brain requires a constant supply of oxygen and glucose to drive ATP production, mostly from oxidative phosphorylation [11]. Neurovascular coupling is assumed to be necessary to increase the supply of energy substrates (oxygen and glucose) in the blood when neurons are active. In fact, the supply of oxygen during neurovascular coupling is substantially greater than that consumed by active brain regions (e.g. [12–15]), at least in the neocortex, resulting in the decrease in deoxygenated haemoglobin that produces the positive BOLD signal commonly measured in fMRI studies [16]. The reason for this oversupply of oxygen remains unclear, but may involve a requirement for a large concentration gradient between the vessel and the tissue for adequate oxygen delivery [17], and the spread of hyperaemia (increased blood supply) to vessels in regions that are not themselves active but that surround and are upstream of active brain regions (see below). Alternatively, the main purpose of neurovascular coupling may not be to increase oxygen supply [18,19] but something else, such as the maintenance of stable tissue glucose concentrations to support aerobic glycolysis [20] (but also see [21,22]), washout of waste products such as CO_2 (but see [23]) and lactate (discussed in [24]), maintenance of appropriate tissue $[O_2]$/$[CO_2]$ ratio [25] or temperature regulation [26]. Whatever its purpose, the regional increase in oxygenated blood generated by neurovascular coupling is reliable enough, in healthy physiology, to generally allow an inference of increased neuronal activity from BOLD fMRI signals. However, an understanding of which cells drive the increase in cerebral blood flow (CBF, figure 1) and which cells consume oxygen is required to fully and accurately interpret BOLD signals and to understand the limits of their utility.

(b) Neuronal subtypes

Neuronal activity is the initiator of the BOLD signal, which is often assumed to represent the aggregate activity of excitatory neurons in a brain region. Indeed, task-associated BOLD signals increase in areas of the brain where the excitatory activity is expected to be increasing [27–30]. Furthermore, studies combining electrophysiological recordings or specific inhibitors of neural activity with BOLD signals [30] and haemodynamic increases [31,32] have directly demonstrated that these measures reflect an underlying increase in net neural activity. Conversely, negative BOLD responses in human subjects were observed in regions exhibiting increased GABAergic tone [33], and thus where neuronal activity may have decreased below baseline levels. The idea that increased inhibition, and thus lower net neural activity, underlies negative BOLD responses is further supported by experiments in primates [34] and rodents [35–38], which show that negative BOLD and haemodynamic signals occur in areas with decreased excitatory activity [39]. While this simple interpretation, that positive and negative BOLD signals reflect increases and decreases in net activity, lends itself easily to investigations of cognitive function in humans, it may not always hold true. Pharmacological studies blocking both glutamate and γ-aminobutyric acid (GABA) receptors have shown that both neurotransmitters are likely involved in neurovascular coupling [32,40,41], suggesting that haemodynamic responses (and, therefore, the BOLD signal) are elicited by a combination of signals from excitatory and inhibitory neurons. Indeed, inhibitory interneurons may play a more important role in the production of BOLD signals than was previously appreciated. Many classes of interneurons have processes that directly target blood vessels [42] and can induce or modify neurovascular coupling [43]. Emerging evidence also indicates that inhibitory neurons can directly alter cerebral haemodynamics [44–48] in a manner that can be independent of net local activity [47,49]. In particular, using an optogenetic approach, Lee *et al*. [47] demonstrated that neuronal nitric oxide synthase (nNOS)-expressing interneurons can drive increases in blood volume with minimal change in net neural activity. Activity in different interneuron populations might also generate the negative BOLD response: optogenetic activation of somatostatin- [47] and parvalbumin- [44,50] expressing interneurons can elicit 'negative' haemodynamic responses. However, the contribution of these interneurons to the BOLD response is ambiguous, with studies reporting their ability to evoke positive [44,46,47], inverted [44,47,50] and delayed positive [46,48] haemodynamic responses. While the relative importance of individual subpopulations of inhibitory interneurons in shaping neurovascular coupling remains an open question, it is clear that these cells can directly modulate CBF and that BOLD signals reflect aspects of both excitatory and inhibitory neuronal activity. Therefore, although BOLD signals indicate changes in neural activity in specific brain regions, they cannot distinguish between increases in inhibitory and excitatory activity (see [51] for an in-depth discussion). Further, interneuron dysfunction is emerging as an important contributor to neurological and psychiatric diseases such as Alzheimer's disease, epilepsy and schizophrenia (see [52–56]), which may alter neurovascular coupling and complicate interpretation of the BOLD response in these patient populations.

Task-induced activations may modulate subjects' attention and arousal via the activity of subcortical projection neurons such as neuromodulatory volume transmission systems (noradrenaline, acetylcholine, dopamine, serotonin, etc.), which also modulate neurovascular coupling [57–59] and the BOLD signal [60–62]. These neuromodulatory systems can alter, independently, the activity of excitatory neurons, inhibitory interneurons, astrocytes and even the vasculature itself, potentially complicating interpretation of BOLD signals during states of altered attention or arousal, or during diseases that affect these systems. A key question is whether the sensitivity of the vasculature to ongoing neural activity is altered by changes in neuromodulatory activity. This appears to be the case for the cholinergic system, as pharmacological or neurotoxic decreases in cholinergic tone weakened the correlation between sensory-evoked

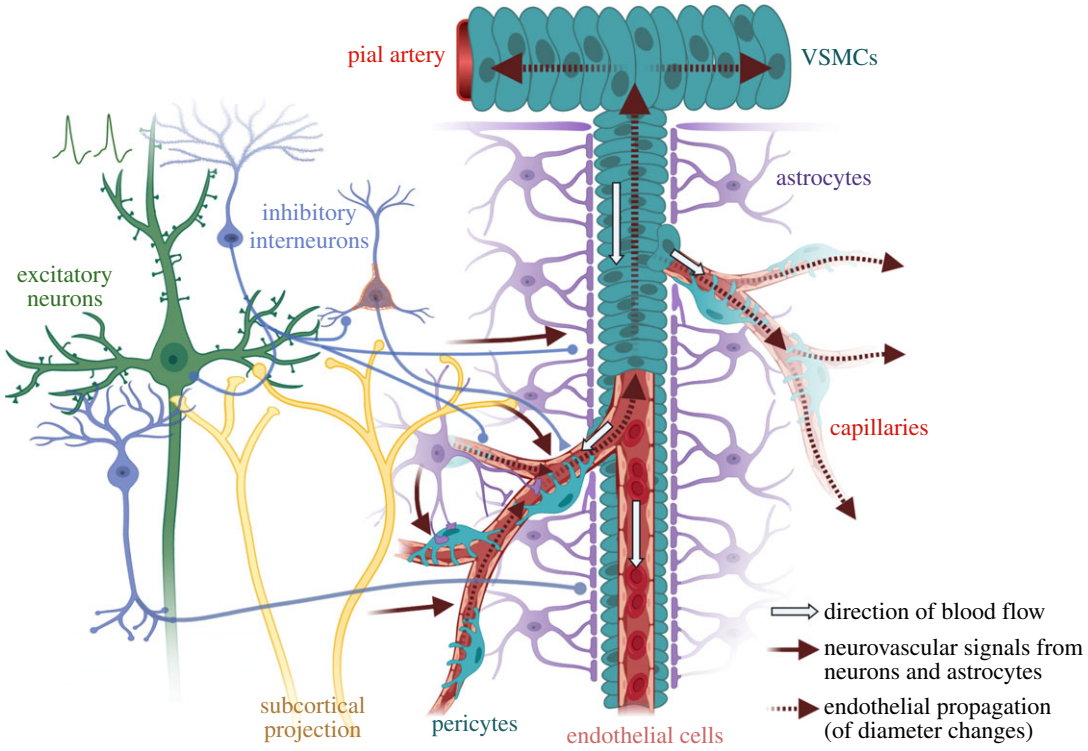

Figure 1. Multicellular contributions to neurovascular coupling. Activation of excitatory neurons in the brain is believed to initiate the neurovascular signals that cause increases in cerebral blood flow (CBF). However, inhibitory interneuron activity almost invariably occurs in parallel with excitatory activity and signals from these interneurons appear to be the stronger regulators of CBF. The neural activity also stimulates astrocytes, which can regulate capillary diameter and modulate overall changes in CBF. Ascending projection systems can further tune the locally generated vasoactive signals, or may directly modulate the vasculature. Once the vascular pericytes or endothelial cells have sensed vasoactive signals from the surrounding tissue, these signals propagate through the endothelium to contractile pericytes and smooth muscle cells on upstream vessels and their branches, which may not themselves feed active tissue. VSMCs, vascular smooth muscle cells. Created with BioRender.com.

neuronal activity and the haemodynamic response [57]. Similar changes may contribute to the impaired neurovascular coupling [63] and BOLD signals [64–66] in Alzheimer's disease, a condition characterized by loss of cholinergic tone [67].

(c) Astrocytes

Astrocytes are in contact with both neuronal synapses and blood vessels, ideally situating them to support neuronal energy demands: either directly through the provision of metabolites such as lactate (reviewed by [68]; see below) or indirectly by involvement in neurovascular coupling (reviewed by [69]).

Neuronal activity can evoke an increase in astrocyte intracellular calcium, leading to the release of vasoactive molecules, and altered haemodynamics [70–74]. Optogenetic stimulation of astrocytes can also increase BOLD without altering neuronal activity [75], indicating that astrocytes *can* act as a bridge between neuronal activity and blood flow. However, astrocytic calcium signals have been criticized as being too slow or infrequent to explain the dilations of arterioles that occur in response to neural activity [70,76–78]. Instead, these slow, usually somatic, increases in astrocyte calcium may: (i) contribute to arteriolar dilation only under conditions of sustained neuronal activity [77,79], (ii) mediate vasoconstriction and the return to baseline tone after functional hyperaemia [80] and (iii) modulate basal vessel tone [77,81,82]. Astrocytes may also facilitate neurovascular coupling, as slow increases in astrocyte calcium may produce longer duration [79] haemodynamic responses.

By contrast to these slow calcium signals, fast calcium signals associated with neural/synaptic activity in (predominantly) astrocytic fine processes and endfeet are increasingly being reported [80,83–85]. These signals occur shortly after neural activity [86,87], precede arteriole and capillary dilation [88] and potentiate the increase in blood volume by almost threefold [80]. These fast signals may be particularly important for controlling flow in the capillary bed, where (unlike in arterioles) astrocyte calcium signals were found to be necessary for neurovascular coupling [71,72].

In summary, astrocytes may drive neurovascular coupling in two ways: fast calcium signals that fine-tune the haemodynamic response by generating molecules that dilate capillaries, and slow calcium signals that modulate the size and shape of arterial dilations, and perhaps help terminate functional hyperaemia when neuronal activity ceases. The specific features of neuronal activity that drive these different astrocyte signals are currently unclear, and their discovery will be key for fully understanding what information haemodynamic and BOLD signals carry about neuronal activity changes. Furthermore, because spin-echo signals reflect changes in capillaries more robustly than gradient echo signals, particularly at higher magnetic fields [89–91], and because capillary dilations depend on fast astrocyte signals, fMRI experiments may differentially reflect certain aspects of neuronal and astrocyte activity depending on the methodology used.

Lastly, the role of astrocytes in shaping the BOLD signal in neurological diseases must also be considered. In Alzheimer's disease and following ischaemia, subarachnoid haemorrhage, and traumatic brain injury, impairments in neurovascular coupling and cerebral haemodynamics have

been reported in both humans and animal models [92,93]. These same conditions are also characterized by reactive astrogliosis, a response of astrocytes to alterations in their microenvironment that includes changes in their morphology and gene expression. It is conceivable that reactive astrocytes are, at least in part, to blame for the neurovascular deficits in these conditions [92,94] and should be the focus of future research. For example, subarachnoid haemorrhage causes an inversion of neurovascular coupling, whereby increases in neural activity are coupled to a decrease in CBF, which is mediated by pathologically large calcium signals within astrocyte endfeet causing a large outflux of potassium, via large conductance calcium-activated potassium (BK) channels, onto the vasculature [95]. Interpretation of the BOLD response from patient populations should, therefore, consider such astrocyte-mediated uncoupling between neural activity and CBF.

(d) The vasculature

In addition to signals from neurons and astrocytes, properties of the vasculature itself shape the BOLD response in multiple ways. While anatomical differences in vascular beds (geometry relative to the magnetic field, vascular density, proportion of veins and capillaries) can alter the magnitude of the BOLD signal (see [1,17,96,97]), we focus here on the contributions of different cell types to the physiological processes that underpin BOLD.

(i) Vascular mural cells: pericytes and smooth muscle cells

The cells that directly constrict and dilate blood vessels by contracting or relaxing in response to signals from the parenchyma, or the blood, are the contractile vascular mural cells: smooth muscle cells (SMCs) and pericytes. The definitions of these two types of cells have been hotly debated [98,99], but here we consider pericytes as mural cells with discrete soma and processes, and SMCs as cells with a banded and contiguous morphology [99]. SMCs on arterioles have long been known to be involved in mediating vascular dilations that underlie neurovascular coupling, whereas the role of pericytes on capillaries and precapillary arterioles has emerged more recently [72,100–102]. Pericyte morphology varies down the vascular bed, as has been elegantly described [103], from ensheathing pericytes, whose processes encircle the underlying vessel, to thin strand pericytes in the middle of the capillary bed, with long processes that extend along but rarely around the vessel. It is now well-established that ensheathing pericytes express smooth muscle actin and can actively constrict and dilate in response to neuronal activity [98,101,103,104]. More controversial is whether mesh and thin strand pericytes on smaller capillaries can regulate vessel diameter. Although some groups find they do not [98,105], neuronal activation causes calcium to drop in these cells [104], and we and others have observed capillary dilations in response to neuronal activity (up to fourth branching order, diameter ≤ 5 µm [72,101,102,104,106]), and two recent papers report constriction of mid-capillary pericytes in response to optogenetic stimulation [107,108]. We suspect that the imaging resolution, sampling rate and smoothing may be key factors in whether these small fluctuations in diameter in the mid-capillary bed can be detected. The evolutionary reason for such local regulation of blood flow is unclear. Perhaps active neurons' oxygen requirements are best matched by very local modulation of blood flow, or perhaps local regulation is simply a consequence of local production of vasoactive signalling molecules with a limited diffusional spread. Alternatively, capillary-level regulation of flow could optimize tissue oxygenation by mediating the increase in homogeneity of red blood cell flux in different capillaries that happens during functional activation [109,110], which maximizes oxygen extraction [111,112].

The responses of all of these different types of pericytes are important for shaping the increase in CBF that occurs following neuronal activity. Because capillaries represent a higher resistance to flow than arterioles or venules [113], their dilation produces a larger decrease in resistance than does arteriole dilation. Therefore, relaxation of capillary pericytes mediates a larger component of the functional hyperaemia response (capillary dilation contributes to 50–84% of the overall change in CBF, while arteriole dilation contributes less than 25% [101,104]). The speed at which different types of pericytes respond to neuronal activation varies, with ensheathing pericytes on the first and second branches off an arteriole dilating before downstream mid-capillary pericytes [101,104,114]. The relative response times of first-order branches compared with upstream arterioles is less clear, with different studies reporting that first-order branches dilate earlier than [101,114], concurrently with [104] or following [115,116] the upstream arterioles. Regardless of timing, these dilations are functionally important: using a compartmentalized computational model, Rungta *et al.* [104] demonstrated that the absence of dilation by either ensheathing or mid-capillary pericytes profoundly attenuates evoked increases in CBF. Thus, the BOLD signal is shaped in different ways by ensheathing pericytes—the likely initiators of capillary dilation—and mid-capillary thin strand pericytes, whose dilation mediates the majority of the increase in flow.

These vascular mural cells might also be differentially sensitive to disease. For example, in Alzheimer's disease, soluble amyloid β (Aβ) constricts pericytes [117], whereas its effect on SMCs is more debated [117–119]. Cerebral amyloid angiopathy, on the other hand, in which Aβ aggregates deposit on vessels, preferentially occurs around the SMCs of larger arterioles [120] and restricts their function [121]. Thus, BOLD signals in patients with Alzheimer's disease might be compromised differently depending on the disease state, owing to effects initially on pericytes by soluble Aβ, and later on SMCs by aggregates of Aβ that form around arterioles.

(ii) Endothelial cells

The best-established role of endothelial cells in shaping the vascular response to neuronal activity, and therefore the BOLD signal, is to propagate vasodilatory signals along the vasculature, thus amplifying the haemodynamic response by dilating blood vessels upstream of local neural activity. Such long-range propagation and modulation of blood flow has long been known to occur in peripheral vascular beds [122,123], the retina [124] and the brain [125], although the mechanisms that underlie this propagation and how this shapes neurovascular coupling have only recently been appreciated [126,127]. Vasodilation arising from neuronal activity local to the mid-capillary bed can be communicated to upstream vessels by a regenerating hyperpolarizing current that is mediated by Kir2.1 channels [105] and propagated between endothelial cells via connexin-40-containing

gap junctions [128], which couple more efficiently and preferentially with upstream vessels during functional activation [129]. Activation of endothelial NMDA receptors and endothelial NOS (eNOS) can also evoke dilation in adjacent vascular mural cells [130,131]. Given the evidence discussed in previous sections, it is likely that these signals first produce vasodilation in ensheathing pericytes of small arterioles or first capillary branches before being propagated upstream to dilate larger penetrating and pial arterioles. Whether dilation of mid-capillary pericytes occurs as a slowly developing response to the same vasoactive signal that generates a propagating hyperpolarization of endothelial cells, or as a secondary passive response to the upstream dilation, remains to be seen.

Vasoactive signals propagated through the endothelium shape functional hyperaemia, and therefore BOLD signals. The haemodynamic response to neural activity (particularly in the first 10 s of a 12 s hindpaw stimulation) was reduced when endothelial signalling and, therefore, propagation of vasodilation, was prevented by light–dye treatment of pial arteries [132]. Endothelial propagation also gives rise to another interesting phenomenon: once vasodilation has spread upstream to pial arteries, it can then propagate down other vessel branches that feed nearby brain regions that do not themselves harbour any change in neuronal activity [133,134], leading to two important features of the BOLD signal. First, the early haemodynamic response (less than 2 s) is more spatially confined to the active region of the brain compared with the later component, as the signal has not had time to propagate outside the active region [135]. Second, the propagated increase in blood flow is likely to be a major reason why the positive BOLD signal exists: inactive tissue near activated regions experiences an increase in blood supply without any oxygen consumption, allowing the oxygenated haemoglobin levels to increase and deoxyhaemoglobin levels to fall, thereby generating the positive BOLD signal. This idea is supported by optical intrinsic imaging and spectroscopic studies that identified a small region of tissue hypoxia and increased oxygen consumption in the active region, immediately before oxygenated blood volume increased in the surrounding area spanning several millimetres [136,137]. This localized increase in oxygen consumption prior to the CBF increase gives rise to the 'initial dip' sometimes observed in the BOLD signal with a similar spatial and temporal pattern [135,138–140].

BOLD signals can also be shaped by multiple factors that modulate endothelial propagation of vasodilation. In the retina, endothelial conduction is dramatically reduced by the vasoconstricting hormone angiotensin II [141], and facilitated by nitric oxide (NO) [129]. In the cortex, neurovascular coupling depends on arterial endothelial cell caveolae, which may be required to cluster the ion channels needed for propagation [142]. Endothelial propagation may also be modulated by changes in levels of the membrane phospholipid PIP_2 which, when depleted by activation of G_q-coupled receptors, reduce the activity of Kir2.1 and impair propagation of vasodilation [143]. Many of these pathways are modified by disease. Loss of endothelial or pericyte–endothelial gap junction coupling is observed in diabetes [124,129,144], while angiotensin II levels are raised in hypertension [141] and angiotensin II synthesis and its receptor are primary targets of hypertension treatment [145]. These pathologies, or treatments thereof, are likely to regulate endothelial cell coupling and thus the spread of dilation through the vascular network, ultimately influencing the size and shape of the BOLD response. Consideration of impaired functioning of pericytes, SMCs and endothelial cells is, therefore, critical when conducting BOLD experiments in ageing and patient populations.

3. Contributions of metabolism to BOLD signals

As discussed above, the increase in CBF that irrigates active brain regions occurs in response to concerted signalling from several cell types, including excitatory neurons, inhibitory neurons and astrocytes. Haemodynamic responses are further shaped by modulation from subcortical structures, and endothelial propagation along the vascular tree. However, the BOLD response represents not only the increase in oxygenated blood but its balance with the rate of oxygen consumption by nearby cells. Therefore, it is important to consider the oxygen consumption of different cell types in the brain to determine their relative impact on the BOLD signal. Neglecting any roles in increasing blood flow, highly oxygen-consuming cells will reduce blood oxygenation and the positive BOLD signal, so using positive BOLD as a readout of neuronal activity will underrepresent these signals compared with active, but less oxygen-consuming cells. These cells' activity will be better detected using calibrated BOLD methods, which allow the calculation of regional oxygen consumption rates by disambiguating changes in CBF from the BOLD response [146].

(a) Excitatory neurons

Energy budgets of neuronal transmission, which calculate the expected ATP use of different cellular processes based on membrane conductances, firing rates and sizes of different cell types, initially suggested that action potentials accounted for the largest proportion of signalling energy use within rodent cortical grey matter [4]. However, incorporating energetically efficient action potentials [147,148] into such calculations results in excitatory synapses being the most energetically expensive component of neuronal signalling [5]. This is because of the relatively large ion fluxes that drive excitatory post-synaptic potentials (EPSPs) compared with action potentials, which then need to be reversed by the action of the sodium–potassium ATPase. The proportion of energy use associated with various cortical signalling processes has been suggested to be consistent across mammalian species and activity levels, with post-synaptic processes being the largest consumers of neuronal ATP in both rodents (47–53%) and humans (42–59%) [149]. These findings support the use of rodent models in fMRI studies informing our knowledge of human brain function. Careful cross-species approaches will allow more reliable translation of findings between preclinical and human fMRI studies [150].

ATP at synapses is proposed to be glycolytically generated [151], and therefore not to consume oxygen or influence the BOLD signal. However, measurements of oxygen concentrations during inhibition of glutamatergic synapses showed that most oxygen was consumed by EPSPs at synapses, followed by action potentials [11], and that the correlations between local field potentials and cerebral metabolic rate of O_2 ($CMRO_2$) [152,153] support excitatory synapses as a crucial determinant of $CMRO_2$. Because there are nine times more excitatory than inhibitory neurons in the cerebral cortex

[154] and because excitatory neurons have more excitatory synapses than do interneurons [155], much of the oxygen consumed by EPSPs and action potentials will be used by excitatory cells. Hence, it follows that excitatory neurons are a major consumer of tissue oxygen.

(b) Inhibitory neurons

While fewer in number, inhibitory neurons may still contribute to brain oxygen consumption in two substantial ways: first, by increasing the energetic cost of excitation and second, by being, on average, more metabolically active than excitatory neurons [156].

Inhibitory inputs can increase the energetic costs of excitatory cells' firing. Reversal of chloride fluxes at inhibitory synapses is, in itself, not expected to be energetically expensive as the reversal potential for chloride is near the resting membrane potential of the cell. However, the co-occurrence of excitation and inhibition may increase the energetic cost of excitation in at least two ways. Firstly, inhibition increases the metabolic cost of excitatory synapses: by holding the membrane at more hyperpolarized potentials, inhibition increases the driving force and inward flux of sodium ions, and more ATP is required to reverse these ion fluxes [157]. Secondly, in the presence of inhibition, more excitatory inputs are required for a cell to reach its threshold for firing an action potential. This happens because excitation needs to counter both hyperpolarization of the membrane and shunting inhibition—the increased membrane conductance caused by the opening of chloride or potassium channels that impairs the spread of EPSPs to the axon hillock. The increased sodium driving force and the requirement for more synaptic inputs both critically depend on the timing of inhibitory inputs, with increased temporal overlap between inhibitory and excitatory inputs to a single cell predicted to dramatically impact the energy cost of neuronal transmission [157]. In fact, inhibitory and excitatory inputs to hippocampal and cortical neurons are often near-synchronous during fast sharp-wave ripple [158,159], theta-like [160] and slow (less than 1 Hz) oscillations [161], suggesting that inhibition is likely to increase the energy used to fuel excitatory neurons in these conditions. This 'tight balance' of excitation and marginally delayed inhibition to individual principal neurons is a common (though not universal) feature of neural networks, which increases the precision of spike timing and makes coding more efficient by reducing the number of spikes needed to accurately represent information at the population level [162]. Thus, brain networks may offset increased synaptic energy use caused by concurrent excitation and inhibition with resultant decreased energy spent on spiking per unit of information transmitted.

The degree of overlap of excitation and inhibition is not constant at a synapse, suggesting that the metabolic cost of inhibition will also vary. At CA3–CA1 synapses, Bhatia *et al*. [163] found no overlap between EPSCs and IPSCs in response to activation of only a few synapses, while stronger stimuli evoked faster IPSCs that overlapped with EPSCs. Therefore, inhibition is expected to disproportionately increase synaptic energy use for stronger stimuli in this network, potentially reducing the size of the positive BOLD response to such stimuli (which would be better represented by $CMRO_2$ measurements from calibrated BOLD). Factors that alter inhibition, such as alterations in brain state and the neuromodulators acetylcholine and noradrenaline [164,165], are also likely to affect the degree of overlap of inhibitory and excitatory currents, and therefore the synaptic energy use. The contribution of inhibitory currents to excitatory synaptic energy use is, therefore, likely to be quite variable and altered in different arousal states or disease, but requires quantification before it is possible to estimate its effect on net $CMRO_2$ or BOLD signal.

In addition to the impact of inhibition on the metabolic cost of excitatory synaptic inputs, increased energy use due to inhibition may occur as a result of oxygen consumption by inhibitory interneurons themselves. Fast-spiking parvalbumin interneurons are probably the main contributor to increased energy metabolism during inhibition. They are relatively numerous (around 40% of GABAergic cells in neocortex, for example [166]) and, relative to other interneurons, they have higher levels of cytochrome *c* oxidase, more mitochondria, a higher density of excitatory inputs and adaptations such as increased sodium channel density, which allows an extremely fast firing rate but decreases the energy efficiency of action potential firing [167–169]. The contribution of other interneuron types to net $CMRO_2$ is less studied, but may also be significant (although see [170]), as their firing rates and cytochrome *c* oxidase levels can be higher than those in pyramidal cells [167,168]. By contrast to excitatory neurons, interneurons are generally expected to consume more oxygen to fuel action potentials than synaptic potentials, because of their lower dendritic complexity but increased axonal length and branching [171] (but also see [149]). Notably, the populations of interneurons that are likely to make the largest contribution to brain oxygen consumption may not be the same as those that control blood flow: fast-spiking parvalbumin cells are very metabolically active, but may not play a major role in the control of blood flow, while nNOS-positive interneurons can control blood flow but make up only 20% of all interneurons [42] and 2% of all neurons [172], and hence are likely to be relatively underrepresented in $CMRO_2$. Therefore, positive BOLD and calibrated BOLD $CMRO_2$ measurements provide very different information about which types of inhibitory cells are active.

Experimentally, inhibition has been shown to have a significant energetic cost. 2-Deoxyglucose uptake (and by extrapolation, metabolism) was more correlated with the degree of inhibition than pyramidal cell firing after the electrical stimulation of hippocampal inputs in rats [173]. Similarly, in rat dentate gyrus, low-frequency stimulation of the perforant path decreased EPSP slope and population spike latency (suggesting increased inhibitory tone), and decreased BOLD, but cerebral blood volume was relatively preserved. This indicated that $CMRO_2$ was elevated by the increased inhibition [174]. These studies, therefore, suggest that $CMRO_2$ is not necessarily a good indicator of principal (excitatory) neuron activity, but also represents inhibitory tone, be it altering the metabolic cost of information transmission within excitatory cells and/or the firing of inhibitory neurons themselves.

The impact of inhibition on $CMRO_2$ should make us reconsider the meaning of 'activation' of a brain region. As discussed above, a key function of inhibition is thought to be to increase the precision of spike timing, and it may not necessarily alter the net firing rate of a neuron. Therefore, fluctuations in inhibition during a cognitive process may alter coding and oxygen use in a brain region without altering the

firing rate of principal neurons. From a computational perspective, this brain region is, therefore, involved in the cognitive process but its 'activity' in classic terms of the level of excitatory input or output has not changed. Maybe, then, would it be better to consider that our aim with functional imaging is to detect regions of altered processing, rather than of activation? In this example, where inhibition alters spike timing but not spike rate, $CMRO_2$ measurements would allow us to detect the changes in processing. However, blood flow may not change (depending on whether the interneurons mediating inhibition can dilate vessels) and positive BOLD signal could be increased, decreased or unchanged, depending on the level of any increased energy use and any increase (or not) in CBF.

(c) Glial cells

Metabolism in astrocytes, oligodendrocytes or vascular cells might also be expected to vary with neuronal activity, but, in fact, they probably do not contribute much to the corresponding fluctuations in $CMRO_2$. Astrocytes contain mitochondria and consume oxygen when depolarized optogenetically [75]. However, their metabolism is thought to be predominantly glycolytic [175], and blocking astrocytic oxidative phosphorylation does not affect net $CMRO_2$ [176]. Indeed, active neurons may actually trigger increased glycolytic ATP production in astrocytes to a degree that inhibits astrocytic oxidative phosphorylation, in order to boost oxygen availability for neurons [177]. Lactate produced by glycolysis in astrocytes may then be shuttled to neurons to support their oxidative metabolism [175]. The degree of contribution of this astrocyte–neuron lactate shuttle in fuelling the increased neuronal activity remains controversial [178], however, in part because astrocytic glycolysis occurs after neuronal oxidative phosphorylation [179].

Mature oligodendrocytes consume very little oxygen as their metabolism is predominantly glycolytic, while oligodendrocyte precursor cells (OPCs) produce ATP predominantly via oxidative phosphorylation [180]. However, oxygen use by OPCs associated with increased neuronal activity is likely minimal. Although their resting energy consumption in white matter is similar to that in the grey matter, their activity-dependent ATP use (synaptic connections from axons to OPCs) is less than 1% of the total cost of neuronal signalling in grey matter [181].

(d) Vasculature

The amount of oxygen consumed by the brain's vasculature (endothelial cells, SMCs and pericytes) itself is a question that deserves further study. The maintenance of resting vascular tone, as well as changes therein during neurovascular coupling, are enacted by the movement of ions, particularly calcium and potassium, across the membrane of these vascular cells. ATP is required to re-establish these ionic gradients and, therefore, the vasculature is expected to contribute to metabolism. Experiments performed outside the nervous system suggest that these cells are highly energy consumptive. Sizeable drops in oxygen concentration have been recorded across the vessel wall of mesenteric and pial arteries, and models suggest this reflects significant oxygen consumption by smooth muscle and endothelial cells rather than just the existence of a diffusion barrier [182,183]. Studies in dog and pig aorta have found a significantly higher rate of oxygen consumption at the luminal/endothelial surface compared with the abluminal surface (0.36 versus 0.016 mM min^{-1} [184]), indicating that endothelial cells contribute significantly to vascular consumption rates. The drop in oxygen concentration across the vessel wall also increases with increased wall thickness, or decreasing branching order of the vessel, suggesting that the number of layers of vascular mural cells also plays a role [183]. At 1–5 mM min^{-1} O_2, net $CMRO_2$ of the brain [185,186] is much higher than the oxygen consumption rate of the vasculature measured by some groups [184], though others find higher values (up to 10 mM min^{-1} [182]). However, because the volume fraction of the brain's vasculature is only 1–3% [187], the contribution of vascular cells to net $CMRO_2$ is likely minimal compared with that of neurons, though it may significantly affect O_2 concentrations close to vessels.

In summary, brain oxygen consumption is predominantly due to excitatory and inhibitory neuronal activity, although glial and vascular cells also contribute. Oxygen consumption by active neurons reduces positive BOLD signals, confounding the accuracy of positive BOLD response as a readout of neuronal activity. $CMRO_2$ measurements from calibrated BOLD studies may be a more accurate readout of the level of net neuronal activity than positive BOLD, as they are more spatially localized to active brain regions. However, because the cells that are the most metabolically active (excitatory neurons or parvalbumin interneurons) are likely not the same cells that signal to blood vessels to dilate (likely nNOS-positive inhibitory neurons or astrocytes), $CMRO_2$ signals carry different information about which cells are active compared with positive BOLD signals.

4. Conclusion

BOLD signals are shaped by the balance between oxygen supply and its consumption. Extracting the maximum amount of accurate information from BOLD signals will require understanding which cells' activity shapes these two processes, especially as the same cells are not equally responsible for both processes. The neuronal populations that consume the most oxygen are likely to be different from those that drive the largest increases in CBF. Astrocytes can initiate vascular responses at smaller vessels while modulating the response of arterioles, and vascular mural and endothelial cells detect and propagate these signals to amplify the haemodynamic response ultimately measured by the BOLD response, without contributing as much to oxygen consumption. A nuanced understanding of how alterations in excitatory–inhibitory balance and different interneuron populations affect oxygen supply and consumption is key to discovering how BOLD signals relate to circuit activity. Furthermore, the future interpretation of BOLD signals should also reflect our increasing understanding of how neurons, astrocytes and vascular cells can be differentially affected by disease states, and have correspondingly different effects on the BOLD signal.

Data accessibility. This article has no additional data.

Authors' contributions. All authors contributed equally to this manuscript.

Competing interests. We declare we have no competing interests.

Funding. C.H. is funded by a Sir Henry Dale Fellowship jointly funded by the Wellcome Trust and the Royal Society (grant no. 105586/Z/14/Z). A.M. is funded by Collins Medical Trust, NIH NINDS

(grant no. 1R01NS110690), NIH NIMH (grant no. 1R01DA047237) and NIH NIA (grant no. P30AG066518-01; Oregon Alzheimer's Disease Research Center, PI: Kaye). C.N.H. is funded by the Medical Research Council (grant no. MR/S026495/1), the Royal Society (grant no. RGS\R1\191203) and the Alzheimer's Research UK South Coast Network.

References

1. Gagnon L *et al*. 2015 Quantifying the microvascular origin of BOLD-fMRI from first principles with two-photon microscopy and an oxygen-sensitive nanoprobe. *J. Neurosci.* **35**, 3663–3675. (doi:10.1523/JNEUROSCI.3555-14.2015)
2. Das A, Murphy K, Drew PJ. 2021 Rude mechanicals in brain haemodynamics: non-neural actors that influence blood flow. *Phil. Trans. R. Soc. B* **376**, 20190635. (doi:10.1098/rstb.2019.0635)
3. Sokoloff L. 1960 The metabolism of the central nervous system in vivo. In *Handbook of physiology, I, neurophysiology*, vol. 3 (eds J Field, HW Magoun, VE Hall), pp. 1843–1864. Washington, DC: American Physiological Society.
4. Attwell D, Laughlin SB. 2001 An energy budget for signaling in the grey matter of the brain. *J. Cereb. Blood Flow Metab.* **21**, 1133–1145. (doi:10.1097/00004647-200110000-00001)
5. Howarth C, Gleeson P, Attwell D. 2012 Updated energy budgets for neural computation in the neocortex and cerebellum. *J. Cereb. Blood Flow Metab.* **32**, 1222–1232. (doi:10.1038/jcbfm.2012.35)
6. Oe Y, Baba O, Ashida H, Nakamura KC, Hirase H. 2016 Glycogen distribution in the microwave-fixed mouse brain reveals heterogeneous astrocytic patterns. *Glia* **64**, 1532–1545. (doi:10.1002/glia.23020)
7. Wasserman DH. 2009 Four grams of glucose. *Am. J. Physiol. Endocrinol. Metab.* **296**, E11–E21. (doi:10.1152/ajpendo.90563.2008)
8. Molina DK, DiMaio VJM. 2012 Normal organ weights in men: part II—the brain, lungs, liver, spleen, and kidneys. *Am. J. Forensic Med. Pathol.* **33**, 368–372. (doi:10.1097/PAF.0b013e31823d29ad)
9. Holmes EG, Holmes BE. 1926 Contributions to the study of brain metabolism: carbohydrate metabolism relationship of glycogen and lactic acid. *Biochem. J.* **20**, 1196–1203. (doi:10.1042/bj0201196)
10. Janssen I, Heymsfield SB, Wang Z, Ross R. 2000 Skeletal muscle mass and distribution in 468 men and women aged 18–88 yr. *J. Appl. Physiol.* **89**, 81–88. (doi:10.1152/jappl.2000.89.1.81)
11. Hall CN, Klein-Flugge MC, Howarth C, Attwell D. 2012 Oxidative phosphorylation, not glycolysis, powers presynaptic and postsynaptic mechanisms underlying brain information processing. *J. Neurosci.* **32**, 8940–8951. (doi:10.1523/jneurosci.0026-12.2012)
12. Fox PT, Raichle ME. 1986 Focal physiological uncoupling of cerebral blood flow and oxidative metabolism during somatosensory stimulation in human subjects. *Proc. Natl Acad. Sci. USA* **83**, 1140–1144. (doi:10.1073/pnas.83.4.1140)
13. Lecoq J, Tiret P, Najac M, Shepherd GM, Greer CA, Charpak S. 2009 Odor-evoked oxygen consumption by action potential and synaptic transmission in the olfactory bulb. *J. Neurosci.* **29**, 1424–1433. (doi:10.1523/JNEUROSCI.4817-08.2009)
14. Parpaleix A, Houssen YG, Charpak S. 2013 Imaging local neuronal activity by monitoring PO_2 transients in capillaries. *Nat. Med.* **19**, 241–246. (doi:10.1038/nm.3059)
15. Sakadzić S, Yuan S, Dilekoz E, Ruvinskaya S, Vinogradov SA, Ayata C, Boas DA. 2009 Simultaneous imaging of cerebral partial pressure of oxygen and blood flow during functional activation and cortical spreading depression. *Appl. Opt.* **48**, D169–D177. (doi:10.1364/AO.48.00D169)
16. Ogawa S, Lee TM, Kay AR, Tank DW. 1990 Brain magnetic resonance imaging with contrast dependent on blood oxygenation. *Proc. Natl Acad. Sci. USA* **87**, 9868–9872. (doi:10.1073/pnas.87.24.9868)
17. Buxton RB. 2010 Interpreting oxygenation-based neuroimaging signals: the importance and the challenge of understanding brain oxygen metabolism. *Front. Neuroenerget.* **2**, 8. (doi:10.3389/fnene.2010.00008)
18. Mintun MA, Lundstrom BN, Snyder AZ, Vlassenko AG, Shulman GL, Raichle ME. 2001 Blood flow and oxygen delivery to human brain during functional activity: theoretical modeling and experimental data. *Proc. Natl Acad. Sci. USA* **98**, 6859–6864. (doi:10.1073/pnas.111164398)
19. Lindauer U *et al*. 2010 Neurovascular coupling in rat brain operates independent of hemoglobin deoxygenation. *J. Cereb. Blood Flow Metab.* **30**, 757–768. (doi:10.1038/jcbfm.2009.259)
20. Fox PT, Raichle ME, Mintun MA, Dence C. 1988 Nonoxidative glucose consumption during focal physiologic neural activity. *Science* **241**, 462–464. (doi:10.1126/science.3260686)
21. Powers WJ, Hirsch IB, Cryer PE. 1996 Effect of stepped hypoglycemia on regional cerebral blood flow response to physiological brain activation. *Am. J. Physiol.* **270**, H554–H559. (doi:10.1152/ajpheart.1996.270.2.h554)
22. Angleys H, Østergaard L, Jespersen SN. 2015 The effects of capillary transit time heterogeneity (CTH) on brain oxygenation. *J. Cereb. Blood Flow Metab.* **35**, 806–817. (doi:10.1038/jcbfm.2014.254)
23. Pinard E, Tremblay E, Ben-Ari Y, Seylaz J. 1984 Blood flow compensates oxygen demand in the vulnerable CA3 region of the hippocampus during kainate-induced seizures. *Neuroscience* **13**, 1039–1049. (doi:10.1016/0306-4522(84)90287-2)
24. Raichle ME. 1998 Behind the scenes of functional brain imaging: a historical and physiological perspective. *Proc. Natl Acad. Sci. USA* **95**, 765–772. (doi:10.1073/pnas.95.3.765)
25. Buxton RB. 2021 The thermodynamics of thinking: connections between neural activity, energy metabolism and blood flow. *Phil. Trans. R. Soc. B* **376**, 20190624. (doi:10.1098/rstb.2019.0624)
26. Sukstanskii AL, Yablonskiy DA. 2006 Theoretical model of temperature regulation in the brain during changes in functional activity. *Proc. Natl Acad. Sci. USA* **103**, 12 144–12 149. (doi:10.1073/pnas.0604376103)
27. Logothetis NK, Guggenberger H, Peled S, Pauls J. 1999 Functional imaging of the monkey brain. *Nat. Neurosci.* **2**, 555–562. (doi:10.1038/9210)
28. Marota JJ, Ayata C, Moskowitz MA, Weisskoff RM, Rosen BR, Mandeville JB. 1999 Investigation of the early response to rat forepaw stimulation. *Magn. Reson. Med.* **41**, 247–252. (doi:10.1002/(SICI)1522-2594(199902)41:2<247::AID-MRM6>3.0.CO;2-U)
29. Silva AC, Lee SP, Yang G, Iadecola C, Kim SG. 1999 Simultaneous blood oxygenation level-dependent and cerebral blood flow functional magnetic resonance imaging during forepaw stimulation in the rat. *J. Cereb. Blood Flow Metab.* **19**, 871–879. (doi:10.1097/00004647-199908000-00006)
30. Logothetis NK, Pauls J, Augath M, Trinath T, Oeltermann A. 2001 Neurophysiological investigation of the basis of the fMRI signal. *Nature* **412**, 150–157. (doi:10.1038/35084005)
31. Berwick J, Johnston D, Jones M, Martindale J, Martin C, Kennerley AJ, Redgrave P, Mayhew JEW. 2008 Fine detail of neurovascular coupling revealed by spatiotemporal analysis of the hemodynamic response to single whisker stimulation in rat barrel cortex. *J. Neurophysiol.* **99**, 787–798. (doi:10.1152/jn.00658.2007)
32. Lecrux C *et al*. 2011 Pyramidal neurons are 'neurogenic hubs' in the neurovascular coupling response to whisker stimulation. *J. Neurosci.* **31**, 9836–9847. (doi:10.1523/JNEUROSCI.4943-10.2011)
33. Northoff G, Walter M, Schulte RF, Beck J, Dydak U, Henning A, Boeker H, Grimm S, Boesiger P. 2007 GABA concentrations in the human anterior cingulate cortex predict negative BOLD responses in fMRI. *Nat. Neurosci.* **10**, 1515–1517. (doi:10.1038/nn2001)
34. Shmuel A, Augath M, Oeltermann A, Logothetis NK. 2006 Negative functional MRI response correlates with decreases in neuronal activity in monkey visual area V1. *Nat. Neurosci.* **9**, 569–577. (doi:10.1038/nn1675)
35. Boorman L, Kennerley AJ, Johnston D, Jones M, Zheng Y, Redgrave P, Berwick J. 2010 Negative blood oxygen level dependence in the rat: a model for investigating the role of suppression in neurovascular coupling. *J. Neurosci.* **30**, 4285–4294. (doi:10.1523/JNEUROSCI.6063-09.2010)

36. Boorman L, Harris S, Bruyns-Haylett M, Kennerley A, Zheng Y, Martin C, Jones M, Redgrave P, Berwick J. 2015 Long-latency reductions in gamma power predict hemodynamic changes that underlie the negative BOLD signal. *J. Neurosci.* **35**, 4641–4656. (doi:10.1523/JNEUROSCI.2339-14.2015)
37. Devor A *et al*. 2007 Suppressed neuronal activity and concurrent arteriolar vasoconstriction may explain negative blood oxygenation level-dependent signal. *J. Neurosci.* **27**, 4452–4459. (doi:10.1523/JNEUROSCI.0134-07.2007)
38. Kastrup A *et al*. 2008 Behavioral correlates of negative BOLD signal changes in the primary somatosensory cortex. *Neuroimage* **41**, 1364–1371. (doi:10.1016/j.neuroimage.2008.03.049)
39. Harel N, Lee S-P, Nagaoka T, Kim D-S, Kim S-G. 2002 Origin of negative blood oxygenation level-dependent fMRI signals. *J. Cereb. Blood Flow Metab.* **22**, 908–917. (doi:10.1097/00004647-200208000-00002)
40. Han K *et al*. 2019 Neurovascular coupling under chronic stress is modified by altered GABAergic interneuron activity. *J. Neurosci.* **39**, 10 081–10 095. (doi:10.1523/JNEUROSCI.1357-19.2019)
41. Shi Y, Liu X, Gebremedhin D, Falck JR, Harder DR, Koehler RC. 2008 Interaction of mechanisms involving epoxyeicosatrienoic acids, adenosine receptors, and metabotropic glutamate receptors in neurovascular coupling in rat whisker barrel cortex. *J. Cereb. Blood Flow Metab.* **28**, 111–125. (doi:10.1038/sj.jcbfm.9600511)
42. Tricoire L, Vitalis T. 2012 Neuronal nitric oxide synthase expressing neurons: a journey from birth to neuronal circuits. *Front. Neural Circuits* **6**, 82. (doi:10.3389/fncir.2012.00082)
43. Cauli B *et al*. 2004 Cortical GABA interneurons in neurovascular coupling: relays for subcortical vasoactive pathways. *J. Neurosci.* **24**, 8940–8949. (doi:10.1523/JNEUROSCI.3065-04.2004)
44. Lee JH *et al*. 2010 Global and local fMRI signals driven by neurons defined optogenetically by type and wiring. *Nature* **465**, 788–792. (doi:10.1038/nature09108)
45. Uhlirova H *et al*. 2016 Cell type specificity of neurovascular coupling in cerebral cortex. *eLife* **5**, e14315. (doi:10.7554/eLife.14315)
46. Krawchuk MB, Ruff CF, Yang X, Ross SE, Vazquez AL. 2020 Optogenetic assessment of VIP, PV, SOM and NOS inhibitory neuron activity and cerebral blood flow regulation in mouse somato-sensory cortex. *J. Cereb. Blood Flow Metab.* **40**, 1427–1440. (doi:10.1177/0271678X19870105)
47. Lee L *et al*. 2020 Key aspects of neurovascular control mediated by specific populations of inhibitory cortical interneurons. *Cereb. Cortex* **30**, 2452–2464. (doi:10.1093/cercor/bhz251)
48. Dahlqvist MK, Thomsen KJ, Postnov DD, Lauritzen MJ. 2019 Modification of oxygen consumption and blood flow in mouse somatosensory cortex by cell-type-specific neuronal activity. *J. Cereb. Blood Flow Metab.* **40**, 2010–2025. (doi:10.1177/0271678X19882787)
49. Anenberg E, Chan AW, Xie Y, LeDue JM, Murphy TH. 2015 Optogenetic stimulation of GABA neurons can decrease local neuronal activity while increasing cortical blood flow. *J. Cereb. Blood Flow Metab.* **35**, 1579–1586. (doi:10.1038/jcbfm.2015.140)
50. Lee J *et al*. In press. Opposed hemodynamic responses following increased excitation and parvalbumin-based inhibition. *J. Cereb. Blood Flow Metab.* (doi:10.1177/0271678X20930831)
51. Logothetis NK. 2008 What we can do and what we cannot do with fMRI. *Nature* **453**, 869–878. (doi:10.1038/nature06976)
52. Marín O. 2012 Interneuron dysfunction in psychiatric disorders. *Nat. Rev. Neurosci.* **2012**, 107–120. (doi:10.1038/nrn3155)
53. Palop JJ, Mucke L. 2016 Network abnormalities and interneuron dysfunction in Alzheimer disease. *Nat. Rev. Neurosci.* **17**, 777–792. (doi:10.1038/nrn.2016.141)
54. Ferguson BR, Gao W-J. 2018 PV interneurons: critical regulators of E/I balance for prefrontal cortex-dependent behavior and psychiatric disorders. *Front. Neural Circuits* **12**, 37. (doi:10.3389/fncir.2018.00037)
55. Zhu Q, Naegele JR, Chung S. 2018 Cortical GABAergic interneuron/progenitor transplantation as a novel therapy for intractable epilepsy. *Front. Cell Neurosci.* **12**, 167. (doi:10.3389/fncel.2018.00167)
56. Dudek FE, Shao L-R. 2003 Loss of GABAergic interneurons in seizure-induced epileptogenesis. *Epilepsy Curr.* **3**, 159–161. (doi:10.1046/j.1535-7597.2003.03503.x)
57. Lecrux C *et al*. 2017 Impact of altered cholinergic tones on the neurovascular coupling response to whisker stimulation. *J. Neurosci.* **37**, 1518–1531. (doi:10.1523/JNEUROSCI.1784-16.2016)
58. Lecrux C, Hamel E. 2016 Neuronal networks and mediators of cortical neurovascular coupling responses in normal and altered brain states. *Phil. Trans. R. Soc. B* **371**, 20150350. (doi:10.1098/rstb.2015.0350)
59. Perrenoud Q, Rossier J, Férézou I, Geoffroy H, Gallopin T, Vitalis T, Rancillac A. 2012 Activation of cortical 5-HT_3 receptor-expressing interneurons induces NO mediated vasodilatations and NPY mediated vasoconstrictions. *Front. Neural Circuits* **6**, 50. (doi:10.3389/fncir.2012.00050)
60. Zaldivar D, Rauch A, Whittingstall K, Logothetis NK, Goense J. 2014 Dopamine-induced dissociation of BOLD and neural activity in macaque visual cortex. *Curr. Biol.* **24**, 2805–2811. (doi:10.1016/j.cub.2014.10.006)
61. Zaldivar D, Rauch A, Logothetis NK, Goense J. 2018 Two distinct profiles of fMRI and neurophysiological activity elicited by acetylcholine in visual cortex. *Proc. Natl Acad. Sci. USA* **115**, E12073–E12082. (doi:10.1073/pnas.1808507115)
62. Rauch A, Rainer G, Logothetis NK. 2008 The effect of a serotonin-induced dissociation between spiking and perisynaptic activity on BOLD functional MRI. *Proc. Natl Acad. Sci. USA* **105**, 6759–6764. (doi:10.1073/pnas.0800312105)
63. Hock C *et al*. 1997 Decrease in parietal cerebral hemoglobin oxygenation during performance of a verbal fluency task in patients with Alzheimer's disease monitored by means of near-infrared spectroscopy (NIRS) — correlation with simultaneous rCBF-PET measurements. *Brain Res.* **755**, 293–303. (doi:10.1016/s0006-8993(97)00122-4)
64. Golby A *et al*. 2005 Memory encoding in Alzheimer's disease: an fMRI study of explicit and implicit memory. *Brain* **128**, 773–787. (doi:10.1093/brain/awh400)
65. Rombouts SA *et al*. 2000 Functional MR imaging in Alzheimer's disease during memory encoding. *Am. J. Neuroradiol.* **21**, 1869–1875.
66. Kato T, Knopman D, Liu H. 2001 Dissociation of regional activation in mild AD during visual encoding: a functional MRI study. *Neurology* **57**, 812–816. (doi:10.1212/WNL.57.5.812)
67. Hasselmo ME, Sarter M. 2011 Modes and models of forebrain cholinergic neuromodulation of cognition. *Neuropsychopharmacology* **36**, 52–73. (doi:10.1038/npp.2010.104)
68. Escartin C, Rouach N. 2013 Astroglial networking contributes to neurometabolic coupling. *Front. Neuroenerget.* **5**, 4. (doi:10.3389/fnene.2013.00004)
69. Attwell D, Buchan AM, Charpak S, Lauritzen M, Macvicar BA, Newman EA. 2010 Glial and neuronal control of brain blood flow. *Nature* **468**, 232–243. (doi:10.1038/nature09613)
70. Winship IR, Plaa N, Murphy TH. 2007 Rapid astrocyte calcium signals correlate with neuronal activity and onset of the hemodynamic response *in vivo*. *J. Neurosci.* **27**, 6268–6272. (doi:10.1523/JNEUROSCI.4801-06.2007)
71. Biesecker KR, Srienc AI, Shimoda AM, Agarwal A, Bergles DE, Kofuji P, Newman EA. 2016 Glial cell calcium signaling mediates capillary regulation of blood flow in the retina. *J. Neurosci.* **36**, 9435–9445. (doi:10.1523/JNEUROSCI.1782-16.2016)
72. Mishra A, Reynolds JP, Chen Y, Gourine AV, Rusakov DA, Attwell D. 2016 Astrocytes mediate neurovascular signaling to capillary pericytes but not to arterioles. *Nat. Neurosci.* **19**, 1619–1627. (doi:10.1038/nn.4428)
73. Schummers J, Yu H, Sur M. 2008 Tuned responses of astrocytes and their influence on hemodynamic signals in the visual cortex. *Science* **320**, 1638–1643. (doi:10.1126/science.1156120)
74. Zonta M, Angulo MC, Gobbo S, Rosengarten B, Hossmann K-A, Pozzan T, Carmignoto G. 2003 Neuron-to-astrocyte signaling is central to the dynamic control of brain microcirculation. *Nat. Neurosci.* **6**, 43–50. (doi:10.1038/nn980)
75. Takata N *et al*. 2018 Optogenetic astrocyte activation evokes BOLD fMRI response with oxygen consumption without neuronal activity modulation. *Glia* **66**, 2013–2023. (doi:10.1002/glia.23454)
76. Nizar K *et al*. 2013 *In vivo* stimulus-induced vasodilation occurs without IP_3 receptor activation and may precede astrocytic calcium increase. *J. Neurosci.* **33**, 8411–8422. (doi:10.1523/JNEUROSCI.3285-12.2013)

77. Institoris Á, Rosenegger DG, Gordon GR. 2015 Arteriole dilation to synaptic activation that is sub-threshold to astrocyte endfoot Ca^{2+} transients. *J. Cereb. Blood Flow Metab.* **35**, 1411–1415. (doi:10.1038/jcbfm.2015.141)
78. Bonder DE, McCarthy KD. 2014 Astrocytic Gq-GPCR-linked IP_3R-dependent Ca^{2+} signaling does not mediate neurovascular coupling in mouse visual cortex *in vivo*. *J. Neurosci.* **34**, 13 139–13 150. (doi:10.1523/JNEUROSCI.2591-14.2014)
79. Schulz K *et al*. 2012 Simultaneous BOLD fMRI and fiber-optic calcium recording in rat neocortex. *Nat. Methods* **9**, 597–602. (doi:10.1038/nmeth.2013)
80. Gu X, Chen W, Volkow ND, Koretsky AP, Du C, Pan Y. 2018 Synchronized astrocytic Ca^{2+} responses in neurovascular coupling during somatosensory stimulation and for the resting state. *Cell Rep.* **23**, 3878–3890. (doi:10.1016/j.celrep.2018.05.091)
81. Kim KJ, Iddings JA, Stern JE, Blanco VM, Croom D, Kirov SA, Filosa JA. 2015 Astrocyte contributions to flow/pressure-evoked parenchymal arteriole vasoconstriction. *J. Neurosci.* **35**, 8245–8257. (doi:10.1523/JNEUROSCI.4486-14.2015)
82. Mehina EMF, Murphy-Royal C, Gordon GR. 2017 Steady-state free Ca^{2+} in astrocytes is decreased by experience and impacts arteriole tone. *J. Neurosci.* **37**, 8150–8165. (doi:10.1523/JNEUROSCI.0239-17.2017)
83. Di Castro MA, Chuquet J, Liaudet N, Bhaukaurally K, Santello M, Bouvier D, Tiret P, Volterra A. 2011 Local Ca^{2+} detection and modulation of synaptic release by astrocytes. *Nat. Neurosci.* **14**, 1276–1284. (doi:10.1038/nn.2929)
84. Otsu Y, Couchman K, Lyons DG, Collot M, Agarwal A, Mallet J-M, Pfrieger FW, Bergles DE, Charpak S. 2015 Calcium dynamics in astrocyte processes during neurovascular coupling. *Nat. Neurosci.* **18**, 210–218. (doi:10.1038/nn.3906)
85. Wang M, He Y, Sejnowski TJ, Yu X. 2018 Brain-state dependent astrocytic Ca^{2+} signals are coupled to both positive and negative BOLD-fMRI signals. *Proc. Natl Acad. Sci. USA* **115**, E1647–E1656. (doi:10.1073/pnas.1711692115)
86. Stobart JL *et al*. 2018 Cortical circuit activity evokes rapid astrocyte calcium signals on a similar timescale to neurons. *Neuron* **98**, 726–735. (doi:10.1016/j.neuron.2018.03.050)
87. Lind BL, Brazhe AR, Jessen SB, Tan FCC, Lauritzen MJ. 2013 Rapid stimulus-evoked astrocyte Ca^{2+} elevations and hemodynamic responses in mouse somatosensory cortex in vivo. *Proc. Natl Acad. Sci. USA* **110**, E4678–E4687. (doi:10.1073/pnas.1310065110)
88. Lind BL, Jessen SB, Lønstrup M, Joséphine C, Bonvento G, Lauritzen M. 2018 Fast Ca^{2+} responses in astrocyte end-feet and neurovascular coupling in mice. *Glia* **66**, 348–358. (doi:10.1002/glia.23246)
89. Uludag K, Müller-Bierl B, Ugurbil K. 2009 An integrative model for neuronal activity-induced signal changes for gradient and spin echo functional imaging. *Neuroimage* **48**, 150–165. (doi:10.1016/s1053-8119(09)70204-6)
90. Ugurbil K. 2016 What is feasible with imaging human brain function and connectivity using functional magnetic resonance imaging. *Phil. Trans. R. Soc. B* **371**, 20150361. (doi:10.1098/rstb.2015.0361)
91. Norris DG. 2012 Spin-echo fMRI: the poor relation? *Neuroimage* **62**, 1109–1115. (doi:10.1016/j.neuroimage.2012.01.003)
92. Petzold GC, Murthy VN. 2011 Role of astrocytes in neurovascular coupling. *Neuron* **71**, 782–797. (doi:10.1016/j.neuron.2011.08.009)
93. Iadecola C. 2017 The neurovascular unit coming of age: a journey through neurovascular coupling in health and disease. *Neuron* **96**, 17–42. (doi:10.1016/j.neuron.2017.07.030)
94. McConnell HL, Li Z, Woltjer RL, Mishra A. 2019 Astrocyte dysfunction and neurovascular impairment in neurological disorders: correlation or causation? *Neurochem. Int.* **128**, 70–84. (doi:10.1016/j.neuint.2019.04.005)
95. Pappas AC, Koide M, Wellman GC. 2015 Astrocyte Ca^{2+} signaling drives inversion of neurovascular coupling after subarachnoid hemorrhage. *J. Neurosci.* **35**, 13 375–13 384. (doi:10.1523/JNEUROSCI.1551-15.2015)
96. Cavaglia M, Dombrowski SM, Drazba J, Vasanji A, Bokesch PM, Janigro D. 2001 Regional variation in brain capillary density and vascular response to ischemia. *Brain Res.* **910**, 81–93. (doi:10.1016/S0006-8993(01)02637-3)
97. Bohn KA *et al*. 2016 Semi-automated rapid quantification of brain vessel density utilizing fluorescent microscopy. *J. Neurosci. Methods* **270**, 124–131. (doi:10.1016/j.jneumeth.2016.06.012)
98. Hill RA, Tong L, Yuan P, Murikinati S, Gupta S, Grutzendler J. 2015 Regional blood flow in the normal and ischemic brain is controlled by arteriolar smooth muscle cell contractility and not by capillary pericytes. *Neuron* **87**, 95–110. (doi:10.1016/j.neuron.2015.06.001)
99. Attwell D, Mishra A, Hall CN, O'Farrell FM, Dalkara T. 2016 What is a pericyte? *J. Cereb. Blood Flow Metab.* **36**, 451–455. (doi:10.1177/0271678X15610340)
100. Peppiatt CM, Howarth C, Mobbs P, Attwell D. 2006 Bidirectional control of CNS capillary diameter by pericytes. *Nature* **443**, 700–704. (doi:10.1038/nature05193)
101. Hall CN *et al*. 2014 Capillary pericytes regulate cerebral blood flow in health and disease. *Nature* **508**, 55–60. (doi:10.1038/nature13165)
102. Kisler K *et al*. 2017 Pericyte degeneration leads to neurovascular uncoupling and limits oxygen supply to brain. *Nat. Neurosci.* **20**, 406–416. (doi:10.1038/nn.4489)
103. Grant RI, Hartmann DA, Underly RG, Berthiaume A-A, Bhat NR, Shih AY. 2019 Organizational hierarchy and structural diversity of microvascular pericytes in adult mouse cortex. *J. Cereb. Blood Flow Metab.* **39**, 411–425. (doi:10.1177/0271678X17732229)
104. Rungta RL, Chaigneau E, Osmanski B-F, Charpak S. 2019 Vascular compartmentalization of functional hyperemia from the synapse to the pia. *Neuron* **101**, 762. (doi:10.1016/j.neuron.2019.01.060)
105. Longden TA *et al*. 2017 Capillary K^+-sensing initiates retrograde hyperpolarization to increase local cerebral blood flow. *Nat. Neurosci.* **20**, 717–726. (doi:10.1038/nn.4533)
106. Shaw K, Bell L, Boyd K, Grijseels DM, Clarke D. 2019 Hippocampus has lower oxygenation and weaker control of brain blood flow than cortex, due to microvascular differences. *bioRxiv*, 835728. (doi:10.1101/835728)
107. Nelson AR, Sagare MA, Wang Y, Kisler K, Zhao Z, Zlokovic BV. 2020 Channelrhodopsin excitation contracts brain pericytes and reduces blood flow in the aging mouse brain *in vivo*. *Front. Aging Neurosci.* **12**, 108. (doi:10.3389/fnagi.2020.00108)
108. Tieu T, McDowell K, Faino A, Kelly A, Shih AY. 2020 Brain capillary pericytes exert a substantial but slow influence on blood flow. *bioRxiv*, 2020.03.26.008763. (doi:10.1101/2020.03.26.008763)
109. Lee J, Wu W, Boas DA. 2016 Early capillary flux homogenization in response to neural activation. *J. Cereb. Blood Flow Metab.* **36**, 375–380. (doi:10.1177/0271678X15605851)
110. Schulte ML, Wood JD, Hudetz AG. 2003 Cortical electrical stimulation alters erythrocyte perfusion pattern in the cerebral capillary network of the rat. *Brain Res.* **963**, 81–92. (doi:10.1016/S0006-8993(02)03848-9)
111. Rasmussen PM, Jespersen SN, Østergaard L. 2015 The effects of transit time heterogeneity on brain oxygenation during rest and functional activation. *J. Cereb. Blood Flow Metab.* **35**, 432–442. (doi:10.1038/jcbfm.2014.213)
112. Li B *et al*. 2019 More homogeneous capillary flow and oxygenation in deeper cortical layers correlate with increased oxygen extraction. *eLife* **8**, e42299. (doi:10.7554/eLife.42299)
113. Blinder P, Tsai PS, Kaufhold JP, Knutsen PM, Suhl H, Kleinfeld D. 2013 The cortical angiome: an interconnected vascular network with noncolumnar patterns of blood flow. *Nat. Neurosci.* **16**, 889–897. (doi:10.1038/nn.3426)
114. Cai C, Fordsmann JC, Jensen SH, Gesslein B, Lønstrup M, Hald BO, Zambach SA, Brodin B, Lauritzen MJ. 2018 Stimulation-induced increases in cerebral blood flow and local capillary vasoconstriction depend on conducted vascular responses. *Proc. Natl Acad. Sci. USA* **115**, E5796–E5804. (doi:10.1073/pnas.1707702115)
115. Tian P *et al*. 2010 Cortical depth-specific microvascular dilation underlies laminar differences in blood oxygenation level-dependent functional MRI signal. *Proc. Natl Acad. Sci. USA* **107**, 15 246–15 251. (doi:10.1073/pnas.1006735107)
116. Kornfield TE, Newman EA. 2014 Regulation of blood flow in the retinal trilaminar vascular network. *J. Neurosci.* **34**, 11 504–11 513. (doi:10.1523/JNEUROSCI.1971-14.2014)
117. Nortley R *et al*. 2019 Amyloid β oligomers constrict human capillaries in Alzheimer's disease via

signaling to pericytes. *Science* **365**, eaav9518. (doi:10.1126/science.aav9518)

118. Dietrich HH, Xiang C, Han BH, Zipfel GJ, Holtzman DM. 2010 Soluble amyloid-β, effect on cerebral arteriolar regulation and vascular cells. *Mol. Neurodegener.* **5**, 15. (doi:10.1186/1750-1326-5-15)
119. Niwa K, Porter VA, Kazama K, Cornfield D, Carlson GA, Iadecola C. 2001 Aβ-peptides enhance vasoconstriction in cerebral circulation. *Am. J. Physiol. Heart Circ. Physiol.* **2001**, H2417–H2424. (doi:10.1152/ajpheart.2001.281.6.h2417)
120. Han BH *et al*. 2008 Cerebrovascular dysfunction in amyloid precursor protein transgenic mice: contribution of soluble and insoluble amyloid-β peptide, partial restoration via γ-secretase inhibition. *J. Neurosci.* **28**, 13 542–13 550. (doi:10.1523/JNEUROSCI.4686-08.2008)
121. Kimbrough IF, Robel S, Roberson ED, Sontheimer H. 2015 Vascular amyloidosis impairs the gliovascular unit in a mouse model of Alzheimer's disease. *Brain* **138**, 3716–3733. (doi:10.1093/brain/awv327)
122. Segal SS. 2015 Integration and modulation of intercellular signaling underlying blood flow control. *J. Vasc. Res.* **52**, 136–157. (doi:10.1159/000439112)
123. Beach JM, McGahren ED, Duling BR. 1998 Capillaries and arterioles are electrically coupled in hamster cheek pouch. *Am. J. Physiol.* **275**, H1489–H1496. (doi:10.1152/ajpheart.1998.275.4.h1489)
124. Oku H, Kodama T, Sakagami K, Puro DG. 2001 Diabetes-induced disruption of gap junction pathways within the retinal microvasculature. *Invest. Ophthalmol. Vis. Sci.* **42**, 1915–1920.
125. Iadecola C, Yang G, Ebner TJ, Chen G. 1997 Local and propagated vascular responses evoked by focal synaptic activity in cerebellar cortex. *J. Neurophysiol.* **78**, 651–659. (doi:10.1152/jn.1997.78.2.651)
126. Guerra G, Lucariello A, Perna A, Botta L, De Luca A, Moccia F. 2018 The role of endothelial Ca^{2+} signaling in neurovascular coupling: a view from the lumen. *Int. J. Mol. Sci.* **19**, 938. (doi:10.3390/ijms19040938)
127. Rosenblum WI. 2018 Endothelium-dependent responses in the microcirculation observed in vivo. *Acta Physiol.* **224**, e13111. (doi:10.1111/apha.13111)
128. Zechariah A *et al*. 2020 Intercellular conduction optimizes arterial network function and conserves blood flow homeostasis during cerebrovascular challenges. *Arterioscler. Thromb. Vasc. Biol.* **40**, 733–750. (doi:10.1161/ATVBAHA.119.313391)
129. Kovacs-Oller T, Ivanova E, Bianchimano P, Sagdullaev BT. 2020 The pericyte connectome: spatial precision of neurovascular coupling is driven by selective connectivity maps of pericytes and endothelial cells and is disrupted in diabetes. *Cell Discov.* **6**, 39. (doi:10.1038/s41421-020-0180-0)
130. Stobart JLL, Lu L, Anderson HDI, Mori H, Anderson CM. 2013 Astrocyte-induced cortical vasodilation is mediated by D-serine and endothelial nitric oxide synthase. *Proc. Natl Acad. Sci. USA* **110**, 3149–3154. (doi:10.1073/pnas.1215929110)
131. Hogan-Cann AD, Lu P, Anderson CM. 2019 Endothelial NMDA receptors mediate activity-dependent brain hemodynamic responses in mice. *Proc. Natl Acad. Sci. USA* **116**, 10 229–10 231. (doi:10.1073/pnas.1902647116)
132. Chen BR, Kozberg MG, Bouchard MB, Shaik MA, Hillman EMC. 2014 A critical role for the vascular endothelium in functional neurovascular coupling in the brain. *J. Am. Heart Assoc.* **3**, e000787. (doi:10.1161/jaha.114.000787)
133. O'Herron P *et al*. 2016 Neural correlates of single-vessel haemodynamic responses *in vivo*. *Nature* **534**, 378–382. (doi:10.1038/nature17965)
134. Jukovskaya N, Tiret P, Lecoq J, Charpak S. 2011 What does local functional hyperemia tell about local neuronal activation? *J. Neurosci.* **31**, 1579–1582. (doi:10.1523/jneurosci.3146-10.2011)
135. Sheth SA *et al*. 2004 Columnar specificity of microvascular oxygenation and volume responses: implications for functional brain mapping. *J. Neurosci.* **24**, 634–641. (doi:10.1523/JNEUROSCI.4526-03.2004)
136. Frostig RD, Lieke EE, Ts'o DY, Grinvald A. 1990 Cortical functional architecture and local coupling between neuronal activity and the microcirculation revealed by in vivo high-resolution optical imaging of intrinsic signals. *Proc. Natl Acad. Sci. USA* **87**, 6082–6086. (doi:10.1073/pnas.87.16.6082)
137. Malonek D, Grinvald A. 1996 Interactions between electrical activity and cortical microcirculation revealed by imaging spectroscopy: implications for functional brain mapping. *Science* **272**, 551–554. (doi:10.1126/science.272.5261.551)
138. Hu X, Yacoub E. 2012 The story of the initial dip in fMRI. *Neuroimage* **62**, 1103–1108. (doi:10.1016/j.neuroimage.2012.03.005)
139. Menon RS, Ogawa S, Hu X, Strupp JP, Anderson P, Uğurbil K. 1995 BOLD based functional MRI at 4 tesla includes a capillary bed contribution: echo-planar imaging correlates with previous optical imaging using intrinsic signals. *Magn. Reson. Med.* **33**, 453–459. (doi:10.1002/mrm.1910330323)
140. Kim DS, Duong TQ, Kim SG. 2000 High-resolution mapping of iso-orientation columns by fMRI. *Nat. Neurosci.* **3**, 164–169. (doi:10.1038/72109)
141. Zhang T, Wu DM, Xu G-Z, Puro DG. 2011 The electrotonic architecture of the retinal microvasculature: modulation by angiotensin II. *J. Physiol.* **589**, 2383–2399. (doi:10.1113/jphysiol.2010.202937)
142. Chow BW, Nuñez V, Kaplan L, Granger AJ, Bistrong K, Zucker HL, Kumar P, Sabatini BL, Gu C. 2020 Caveolae in CNS arterioles mediate neurovascular coupling. *Nature* **579**, 106–110. (doi:10.1038/s41586-020-2026-1)
143. Harraz OF, Longden TA, Hill-Eubanks D, Nelson MT. 2018 PIP_2 depletion promotes TRPV4 channel activity in mouse brain capillary endothelial cells. *eLife* **7**, e38689. (doi:10.7554/eLife.38689)
144. Ivanova E, Kovacs-Oller T, Sagdullaev BT. 2017 Vascular pericyte impairment and connexin43 gap junction deficit contribute to vasomotor decline in diabetic retinopathy. *J. Neurosci.* **37**, 7580–7594. (doi:10.1523/JNEUROSCI.0187-17.2017)
145. Byrd JB, Ram CVS, Lerma EV. 2019 Pharmacologic treatment of hypertension. In *Nephrology secrets*, 4th edn (eds EV Lerma, MA Sparks, JM Topf), pp. 477–482. (doi:10.1016/b978-0-323-47871-7.00078-2)
146. Blockley NP, Griffeth VEM, Buxton RB. 2012 A general analysis of calibrated BOLD methodology for measuring $CMRO_2$ responses: comparison of a new approach with existing methods. *Neuroimage* **60**, 279–289. (doi:10.1016/j.neuroimage.2011.11.081)
147. Alle H, Roth A, Geiger JRP. 2009 Energy-efficient action potentials in hippocampal mossy fibers. *Science* **325**, 1405–1408. (doi:10.1126/science.1174331)
148. Carter BC, Bean BP. 2009 Sodium entry during action potentials of mammalian neurons: incomplete inactivation and reduced metabolic efficiency in fast-spiking neurons. *Neuron* **64**, 898–909. (doi:10.1016/j.neuron.2009.12.011)
149. Yu Y, Herman P, Rothman DL, Agarwal D, Hyder F. 2018 Evaluating the gray and white matter energy budgets of human brain function. *J. Cereb. Blood Flow Metab.* **38**, 1339–1353. (doi:10.1177/0271678X17708691)
150. Barron HC, Mars RB, Dupret D, Lerch JP, Sampaio-Baptista C. 2021 Cross-species neuroscience: closing the explanatory gap. *Phil. Trans. R. Soc. B* **376**, 20190633. (doi:10.1098/rstb.2019.0633)
151. Mercer RW, Dunham PB. 1981 Membrane-bound ATP fuels the Na/K pump. Studies on membrane-bound glycolytic enzymes on inside-out vesicles from human red cell membranes. *J. Gen. Physiol.* **78**, 547–568. (doi:10.1085/jgp.78.5.547)
152. Masamoto K, Vazquez A, Wang P, Kim S-G. 2008 Trial-by-trial relationship between neural activity, oxygen consumption, and blood flow responses. *Neuroimage* **40**, 442–450. (doi:10.1016/j.neuroimage.2007.12.011)
153. Mathiesen C, Caesar K, Thomsen K, Hoogland TM, Witgen BM, Brazhe A, Lauritzen M. 2011 Activity-dependent increases in local oxygen consumption correlate with postsynaptic currents in the mouse cerebellum *in vivo*. *J. Neurosci.* **31**, 18 327–18 337. (doi:10.1523/JNEUROSCI.4526-11.2011)
154. Abeles M. 1991 *Corticonics: neural circuits of the cerebral cortex*. Cambridge, UK: Cambridge University Press.
155. Villa KL, Nedivi E. 2016 Excitatory and inhibitory synaptic placement and functional implications. In *Dendrites: development and disease* (eds K Emoto, R Wong, E Huang, C Hoogenraad), pp. 467–487. Tokyo, Japan: Springer.
156. McCasland JS, Hibbard LS. 1997 GABAergic neurons in barrel cortex show strong, whisker-dependent metabolic activation during normal behavior. *J. Neurosci.* **17**, 5509–5527. (doi:10.1523/JNEUROSCI.17-14-05509.1997)

157. Buzsáki G, Kaila K, Raichle M. 2007 Inhibition and brain work. *Neuron* **56**, 771–783. (doi:10.1016/j.neuron.2007.11.008)
158. Gan J, Weng S-M, Pernía-Andrade AJ, Csicsvari J, Jonas P. 2017 Phase-locked inhibition, but not excitation, underlies hippocampal ripple oscillations in awake mice *in vivo*. *Neuron* **93**, 308–314. (doi:10.1016/j.neuron.2016.12.018)
159. English DF, Peyrache A, Stark E, Roux L, Vallentin D, Long MA. 2014 Excitation and inhibition compete to control spiking during hippocampal ripples: intracellular study in behaving mice. *J. Neurosci.* **34**, 16 509–16 517. (doi:10.1523/JNEUROSCI.2600-14.2014)
160. Royzen F, Williams S, Fernandez FR, White JA. 2019 Balanced synaptic currents underlie low-frequency oscillations in the subiculum. *Hippocampus* **29**, 1178–1189. (doi:10.1002/hipo.23131)
161. Haider B, Duque A, Hasenstaub AR, McCormick DA. 2006 Neocortical network activity *in vivo* is generated through a dynamic balance of excitation and inhibition. *J. Neurosci.* **26**, 4535–4545. (doi:10.1523/JNEUROSCI.5297-05.2006)
162. Denève S, Machens CK. 2016 Efficient codes and balanced networks. *Nat. Neurosci.* **19**, 375–382. (doi:10.1038/nn.4243)
163. Bhatia A, Moza S, Bhalla US. 2019 Precise excitation-inhibition balance controls gain and timing in the hippocampus. *eLife* **8**, e43415. (doi:10.7554/eLife.43415)
164. Betterton RT, Broad LM, Tsaneva-Atanasova K, Mellor JR. 2017 Acetylcholine modulates gamma frequency oscillations in the hippocampus by activation of muscarinic M1 receptors. *Eur. J. Neurosci.* **45**, 1570–1585. (doi:10.1111/ejn.13582)
165. Garcia-Junco-Clemente P, Tring E, Ringach DL, Trachtenberg JT. 2019 State-dependent subnetworks of parvalbumin-expressing interneurons in neocortex. *Cell Rep.* **26**, 2282–2288. (doi:10.1016/j.celrep.2019.02.005)
166. Lee S, Hjerling-Leffler J, Zagha E, Fishell G, Rudy B. 2010 The largest group of superficial neocortical GABAergic interneurons expresses ionotropic serotonin receptors. *J. Neurosci.* **30**, 16 796–16 808. (doi:10.1523/JNEUROSCI.1869-10.2010)
167. Kann O. 2016 The interneuron energy hypothesis: implications for brain disease. *Neurobiol. Dis.* **90**, 75–85. (doi:10.1016/j.nbd.2015.08.005)
168. Gulyás AI, Buzsáki G, Freund TF, Hirase H. 2006 Populations of hippocampal inhibitory neurons express different levels of cytochrome *c*. *Eur. J. Neurosci.* **23**, 2581–2594. (doi:10.1111/j.1460-9568.2006.04814.x)
169. Hu H, Jonas P. 2014 A supercritical density of Na^+ channels ensures fast signaling in GABAergic interneuron axons. *Nat. Neurosci.* **17**, 686–693. (doi:10.1038/nn.3678)
170. Vazquez AL, Fukuda M, Kim S-G. 2018 Inhibitory neuron activity contributions to hemodynamic responses and metabolic load examined using an inhibitory optogenetic mouse model. *Cereb. Cortex* **28**, 4105–4119. (doi:10.1093/cercor/bhy225)
171. Freund TF, Buzsáki G. 1996 Interneurons of the hippocampus. *Hippocampus* **6**, 347–470. (doi:10.1002/(SICI)1098-1063(1996)6:4<347::AID-HIPO1>3.0.CO;2-I)
172. Valtschanoff JG, Weinberg RJ, Kharazia VN, Schmidt HH, Nakane M, Rustioni A. 1993 Neurons in rat cerebral cortex that synthesize nitric oxide: NADPH diaphorase histochemistry, NOS immunocytochemistry, and colocalization with GABA. *Neurosci. Lett.* **157**, 157–161. (doi:10.1016/0304-3940(93)90726-2)
173. Ackermann RF, Finch DM, Babb TL, Engel Jr J. 1984 Increased glucose metabolism during long-duration recurrent inhibition of hippocampal pyramidal cells. *J. Neurosci.* **4**, 251–264. (doi:10.1523/JNEUROSCI.04-01-00251.1984)
174. Angenstein F. 2019 The role of ongoing neuronal activity for baseline and stimulus-induced BOLD signals in the rat hippocampus. *Neuroimage* **202**, 116082. (doi:10.1016/j.neuroimage.2019.116082)
175. Pellerin L, Magistretti PJ. 2009 Glial energy metabolism: overview. In *Encyclopedia of neuroscience* (ed. LR Squire), pp. 783–788. Oxford, UK: Academic Press. (doi:10.1016/b978-008045046-9.01708-3)
176. Macaisa CM *et al*. 2019 Preserved cerebral oxygen metabolism in astrocytic dysfunction: a combination study of ^{15}O-gas PET with ^{14}C-acetate autoradiography. *Brain Sci.* **9**, 101. (doi:10.3390/brainsci9050101)
177. Fernández-Moncada I, Ruminot I, Robles-Maldonado D, Alegría K, Deitmer JW, Barros LF. 2018 Neuronal control of astrocytic respiration through a variant of the Crabtree effect. *Proc. Natl Acad. Sci. USA* **115**, 1623–1628. (doi:10.1073/pnas.1716469115)
178. Nortley R, Attwell D. 2017 Control of brain energy supply by astrocytes. *Curr. Opin Neurobiol.* **47**, 80–85. (doi:10.1016/j.conb.2017.09.012)
179. Kasischke KA, Vishwasrao HD, Fisher PJ, Zipfel WR, Webb WW. 2004 Neural activity triggers neuronal oxidative metabolism followed by astrocytic glycolysis. *Science* **305**, 99–103. (doi:10.1126/science.1096485)
180. Rao VTS *et al*. 2017 Distinct age and differentiation-state dependent metabolic profiles of oligodendrocytes under optimal and stress conditions. *PLoS ONE* **12**, e0182372. (doi:10.1371/journal.pone.0182372)
181. Harris JJ, Attwell D. 2012 The energetics of CNS white matter. *J. Neurosci.* **32**, 356–371. (doi:10.1523/JNEUROSCI.3430-11.2012)
182. Tsai AG, Friesenecker B, Mazzoni MC, Kerger H, Buerk DG, Johnson PC, Intaglietta M. 1998 Microvascular and tissue oxygen gradients in the rat mesentery. *Proc. Natl Acad. Sci. USA* **95**, 6590–6595. (doi:10.1073/pnas.95.12.6590)
183. Duling BR, Kuschinsky W, Wahl M. 1979 Measurements of the perivascular PO_2 in the vicinity of the pial vessels of the cat. *Pflugers Arch. Eur. J. Physiol.* **383**, 29–34. (doi:10.1007/bf00584471)
184. Buerk DG, Goldstick TK. 1982 Arterial wall oxygen consumption rate varies spatially. *Am. J. Physiol.* **243**, H948–H958. (doi:10.1152/ajpheart.1982.243.6.h948)
185. Gould IG, Tsai P, Kleinfeld D, Linninger A. 2017 The capillary bed offers the largest hemodynamic resistance to the cortical blood supply. *J. Cereb. Blood Flow Metab.* **37**, 52–68. (doi:10.1177/0271678X16671146)
186. Huchzermeyer C, Berndt N, Holzhütter H-G, Kann O. 2013 Oxygen consumption rates during three different neuronal activity states in the hippocampal CA3 network. *J. Cereb. Blood Flow Metab.* **33**, 263–271. (doi:10.1038/jcbfm.2012.165)
187. Schmid F, Barrett MJP, Jenny P, Weber B. 2019 Vascular density and distribution in neocortex. *Neuroimage* **197**, 792–805. (doi:10.1016/j.neuroimage.2017.06.046)